EFFECT OF MELT QUENCHING ON METASTABLE EQUILIBRIUM DIAGRAMS

S. I. Ryabtsev[1]*, O. I. Kushnerov[1], V. F. Bashev[2], T. V. Kalinina[2], E. A. Mikita[2], P. O. Galagan[1]

[1] *Oles Honchar Dnipro National University, Dnipro, Ukraine*
[2] *Dniprovsky State Technical University, Kamianske , Ukraine*
**e-mail: siryabts@gmail.com*

The article investigates the influence of high cooling rates during quenching from the melt on the formation of metastable phases and the appearance of metastable equilibrium diagrams. It is shown that with increasing cooling rate, both an increase in the existence region of strongly supersaturated solid solutions and the formation of new metastable phases in binary Fe-P and Sb-Zn alloys are observed. Mechanisms of non-equilibrium crystallization during quenching from the melt are proposed, the influence of large supercooling under high cooling rate conditions on changes in the kinetics of occurring crystallization and the emerging competition during non-equilibrium crystallization of congruent and incongruent phases are demonstrated. The validity of the newly formed metastable phase in the Sb-Zn alloy is confirmed by the correctness of the dependencies of specific atomic volumes of equilibrium phases calculated using Vegard's approximation. The lattice parameters of the emerging stable and metastable phases in the alloys are calculated.

Keywords: metastability, supercooling, quenching from melt, supersaturated solid solution, phase.

Received 21.09.2025; Received in revised form 15.10.2025; Accepted 14.11.2025

1. Introduction

Diagrams of metastable equilibrium indicate the thermodynamic possibility of metastable phase formation in one or another temperature-concentration region. In addition, knowing the established line of metastable equilibrium allows one to have a reference point for determining the driving force for the formation and growth of metastable phases. Therefore, it is very important to know the layout of these lines, i.e. to have a diagram of metastable equilibrium, which will allow finding the reasons for their displacement or non-compliance of real processes of structural formation with the accepted scheme of the arrangement of lines. Determination of the melting temperature of metastable phases, as well as estimation of the level of their metastability, are very important for the construction of diagrams of metastable equilibrium. It should be noted that the melting temperature of the metastable phase means the temperature of its metastable equilibrium with its own melt. In particular, if rapid heating prevents the disintegration of the metastable phase, it must melt at the temperature of its metastable equilibrium with the liquid.

It should also be emphasized that the metastability value is characterized by the difference between the free energies of a metastable phase formation and a mixture of stable phases of the same composition. It is important to note that the amount of the metastable phase recorded in the rapidly cooled samples is not directly dependent on the level of its metastability, since the output of the phase is also determined by the kinetic factors of its nucleation and growth from the liquid and decay already in the solid state. Diagrams of metastable equilibrium in general do not differ from diagrams of stable equilibrium. The difference lies only in the fact that the lines of the stable diagram determine the composition of phases in stable equilibrium, and the lines of the metastable diagram in metastable equilibrium.

The well-known method of quenching from the melt is accompanied by the implementation of new effects useful for practice during crystallization: the formation of highly supersaturated solid solutions (up to the formation of a continuous series of solid solutions), crystallization of new metastable phases and the emergence of a solid amorphous state in alloys [1-7].

Many of these phases have a unique combination of improved physicochemical characteristics.

Therefore, there is a constant need both to obtain new metastable phases and to study their practical properties. The most popular for such studies are phase diagrams with the presence of eutectics in them [4]. In addition, cases of metastable eutectics crystallization are known, primarily these are Fe-P, Sb-Zn alloys, in which, according to [8], stable incongruent phases of Fe_3P and Zn-Sb do not crystallize at all without seeding. As a result, metastable eutectics (α^1 + Fe_3P) and (α^1 + Zn_4Sb_3) are formed in these systems. At the same time, experiments on quenching these alloys from the melt showed that the true situation during nonequilibrium crystallization is significantly more complex than shown in [8] and requires additional research.

2. Experimental details

High-purity (99.9%) elements were used to fabricate the Fe-P and Sb-Zn alloys. First, bulk ingots were produced in a Tamman electric furnace under argon protection with a cooling rate of ~10^2 K/s. These ingots were then subjected to splat-quenching, where the molten droplets were ejected on to the inner wall of a hollow copper cylinder (R=135 mm) rotating at ~8000 rpm. The cooling rate for the films was derived to be ~ 10^6 K/s, determined from the film thickness (δ), heat transfer coefficient (α), density (ρ), and heat capacity (c) as described in references [9–12].

The phase composition and periods of crystal lattices were studied using the diffraction method of the DRON-2.0 X-ray diffractometer in monochromatic copper radiation, the accuracy of determining the lattice period was ±0.0002 nm.

3. Results and discussion

It follows from the obtained results that at all the investigated cooling rates, up to the formation of a solid amorphous state (10^8 K/s) in the composition range from 19 to 25 at. % phosphorus, a mixture of stable phases crystallizes in iron-phosphorus alloys: α-Fe + Fe_3P, and in splat-quenched (SQ) alloys with a phosphorus content of up to 19%, homogeneous highly supersaturated solid solutions are formed. A decrease in the cooling rate to 10^6 K/s leads to a sharp saturation of the solid solution to a value not exceeding the maximum solubility of phosphorus at the eutectic temperature (~4.9%). The excess phase here is the stable phase Fe_3P. The results obtained in the work are not consistent with the data presented in [4]. A possible reason for this may be the final purity of the materials used in melting. Thus, in the work [13], on the basis of precise magnetic measurements and thermal analysis, it is stated that already at a nitrogen content of 0.005 – 0.008 wt.% in the alloy the metastable version of the state diagram is not realized. However, the true reason for this is not exactly known, since the purity of the original materials used is unknown.

Qualitatively new results were obtained in this work in SQ samples with a phosphorus content of 25 to 33%. Thus, on the diffraction patterns of $Fe_{72}P_{28}$ alloy samples with a thickness of 5 – 7 nm, lines of three phases are observed: α-Fe, Fe_3P, Fe_2P, and the phosphorus content in the solid solution based on bcc iron exceeds the maximum solubility at the eutectic temperature and is 6% (a = 0.2861 nm). In SQ alloys $Fe_{70}P_{30}$ the degree of saturation of the solid solution based on BCC iron increases to 8%, which is in agreement with the metastable version of the Fe-P diagram (Fig. 1). During the splat quenching of melts with a phosphorus content of more than 25%, a change in the crystal lattice periods of the congruent phase Fe_2P is observed depending on the composition: thus, for the alloy with 28% P, these changes are: a = 0.3438 nm, c = 0.5918 nm; for the alloy with 30% P: a = 0.3453 nm, c = 0.5890 nm, which indicates the presence of a homogeneity region in this phase. The

following should be noted: in the diffraction patterns of the SQ alloys with 28% P at cooling rates greater than 10^7 K/s, the lines of the incongruent phase Fe_3P have a narrower appearance, which indicates its high growth rate compared to the congruent phase Fe_2P. With a decrease in the cooling rate to 10^6 K/s, the lines of both phases become almost identical.

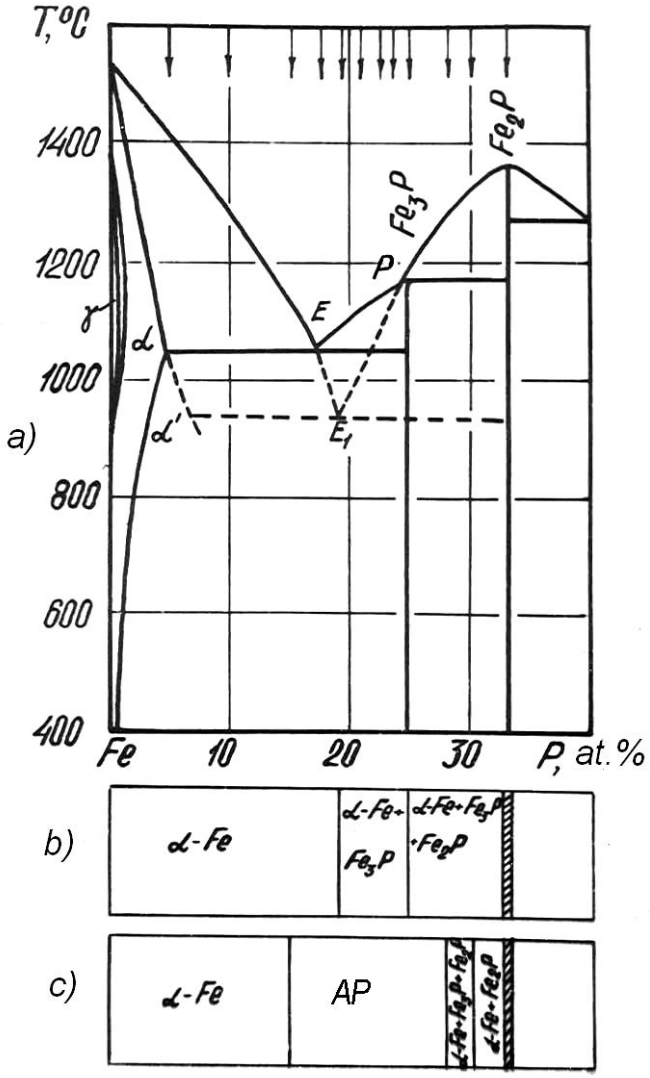

Fig. 1. Fe-P system: a) phase equilibrium diagram (stable – solid lines, metastable – dotted lines), b) phase composition after splat quenching, cooling rate 10^6 K/s, c) the same, 10^8 K/s.

Fe-P phase diagram that interests us ($\alpha^1 + Fe_2P$) is realized at cooling rates of ~ 10^8 K/s only in alloys with a phosphorus content of more than 28%. In this case, the crystallization scheme can be as follows: solidification of the alloy begins with the precipitation of crystals of the Fe_2P phase and, as its amount increases, the composition of the liquid phase changes along the equilibrium liquidus line to the point, when crystallization of the Fe_3P phase becomes possible. However, the latter does not originate in the presence of a congruent phase due to kinetic factors and crystallization continues along the metastable diagram. The composition of the liquid continues to change along the line until the point E_1 is reached, after which the metastable eutectic ($\alpha^1 + Fe_2P$) crystallizes.

A similar crystallization pattern is observed in the Sb-Zn system (Fig. 2). According to the data available in the literature [4], the metastable version of the phase diagram (shown in Fig. 2 by the dotted line) is also realized at normal cooling rates. The stable version of the phase diagram (solid lines) can be realized after introducing ZnSb crystals into the melt as a seed. The experiments conducted in this work during the liquid-liquid reaction of this melt showed that the metastable version of the diagram $Sb+Zn_4Sb_3$ is realized only in alloys containing more than 43.8% Zn. In the right part of the diagram, the metastable version can also be realized: $Zn'+Zn_4Sb_3$ with some expansion of the region of Zn-based solid solutions, as evidenced by the change in the periods of its crystal lattice (*a* from 0.2665 nm to 0.2671 nm and *c* from 0.4947 nm to 0.4981 nm).

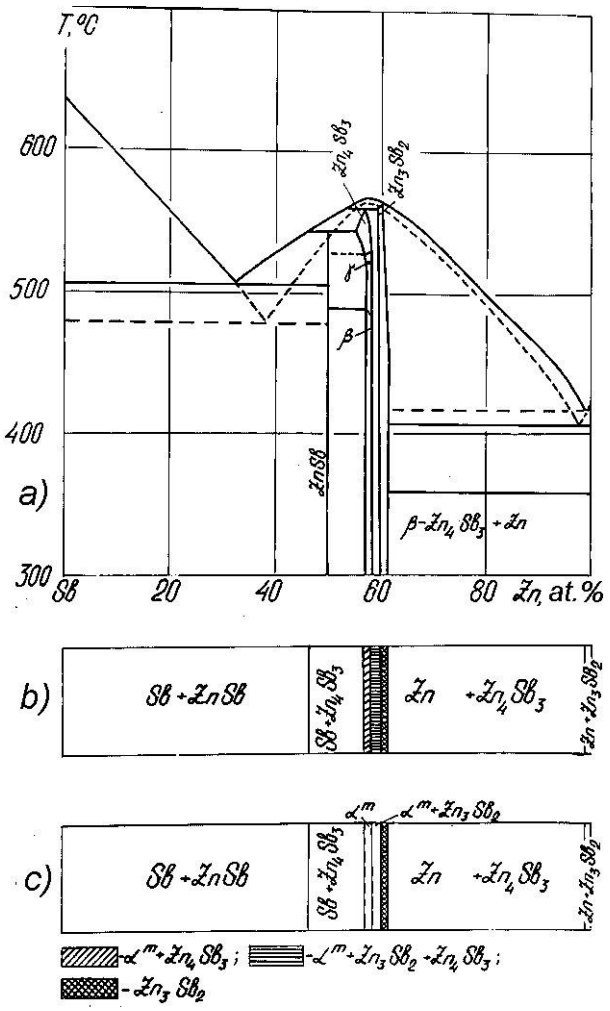

Fig. 2. Zn-Sb system: a) phase equilibrium diagram (stable – solid lines, metastable – dotted lines), b) phase composition after splat quenching, cooling rate 10^6 K/s; c) the same, 10^8 K/s.

A complete summary of the stable and metastable phases obtained in SQ alloys at cooling rates of 10^6-10^8 K/s is shown in Fig. 2. It is interesting to note that on the diffraction patterns of the SQ alloys Sb +(57-58%) Zn at a rate of ~10^8 K/s, lines of a new metastable phase (α^m) with a BCC lattice with a period of a = 0.3941 nm appear, and the volume per atom in the unit cell of this phase is 0.0306 nm^3/at, which correlates quite well with the

dependence of the specific atomic volumes of the equilibrium phases (Sb and Zn), calculated in the Vegard approximation (Fig. 3). Annealing samples with a metastable phase α^m at 300 ºC for 1 min leads to its complete decomposition with the formation of a stable compound Zn_4Sb_3. The formation of this metastable bcc phase of equiatomic composition at splat quenching may indicate significant supercooling of the melt, which results in favorable thermodynamic and kinetic conditions for the formation of a metastable phase in equilibrium with the supercooled liquid. Indirectly, this may also indicate the presence of Sb-Zn clusters with an arrangement of atoms close to BCC in the melt.

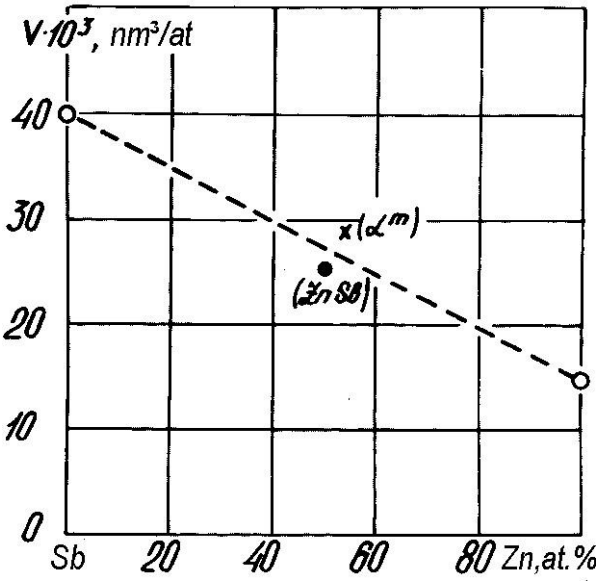

Fig. 3. Dependence of specific atomic volumes of equilibrium and metastable (α^m) phases.

4. Conclusions

1. The work studies in detail the influence of high quenching rates from the alloy on the change in the type of state diagrams and the formation of metastable equilibrium diagrams.

2. The appearance of a new metastable phase with a BCC lattice in the Sb-Zn system has been established, and its periods have been calculated.

3. The expansion of the homogeneity region of the congruent phase Fe_2P is fixed.

References

1. **Brazhkin, V. V.** Metastable phase transformation and phase diagrams in physics and chemistry / V. V. Brazhkin // Phys. Usp. – 2006. – Vol. 49. – P. 719 – 724.

2. **Azarenkov, M. A.** Fazovi rivnovahy i diahramy stanu : navch. posibnyk. Ch. 1 / M. A. Azarenkov, V. Ye. Semenenko, S. V. Lytovchenko. – Kharkiv : KhNU im. V. N. Karazina, 2006. – 100 p.

3. **Tkatch, V. I.** The effect of the melt–spinning processing parameters on the rate of cooling / V. I. Tkatch, A. L. Limanovskii, S. N. Denisenko, S. G. Rassolov // Mater. Sci. Eng. – 2002. – Vol. A323. – P. 91 – 96.

4. **Herlach, D. M.** Metastable materials solidified from undercooled melts / D. M. Herlach // J. Phys. Condens Matter. – 2001. – Vol. 13. – P. 7737 – 7758.

5. **Jones, H.** Developments in aluminium alloys by solidification at higher cooling rates / H. Jones // Aluminium. – 1978. – Vol. 54, No. 4. – P. 274 – 281.

6. **Pogatscher, S.** Solid-solid phase transitions via melting in metals / S. Pogatscher, D. Lentenegger, J. E. K. Schawe, P. J. Uggjwitzer, J. F. Loffler // Nat. Commun. – 2016. – Vol. 7, No. 1. – P. 11113.

7. **Raj, C. R.** Recent developments in thermo-physical property enhancement and applications of solid-solid phase change materials / C. R. Raj, S. Suresh, R. R. Bhavsar, V. K. Singh // J. Therm. and Calorim. – 2020. – Vol. 139, No. 5. – P. 3023 – 3049.

8. **Massalski, T. B.** Binary alloy phase diagrams. Vol. 1 / T. B. Massalski. – Metals Park : Amer. Soc. Met., 1986. – 1115 p.

9. **Bashev, V. F.** Structure and properties of CoCrFeNiMnBe high-entropy alloy films obtained by melt quenching / V. F. Bashev, O. I. Kushnerov, S. I. Ryabtsev // Molecular Crystals and Liquid Crystals. – 2023. – Vol. 765, No. 1. – P. 145 – 153.

10. **Polonskyy, V. A.** Structure and corrosion-electrochemical properties of rapidly quenched Fe5CrCuNiMnSi and Fe5CoCuNiMnSi high entropy alloys / V. A. Polonskyy, V. F. Bashev, O. I. Kushnerov // J. Chem. Technol. – 2022. – Vol. 30. – P. 88 – 95.

11. **Polonskyy, V. A.** The influence of the cooling rate on the structure and corrosion properties of the multicomponent high-entropy alloy CoCrFeNiMnBe / V. A. Polonskyy, O. I. Kushnerov, V. F. Bashev, S. I. Ryabtsev // Physics and Chemistry of Solid State. – 2024. – Vol. 25, No. 3. – P. 506 –512.

12. **Bashev, V. F.** Influence of Liquid Quenching on Phase Composition and Properties of Be-Si Eutectic Alloy / V. F. Bashev, S. I. Ryabtsev, O. I. Kushnerov, N. A. Kutseva, S. N. Antropov // East European Journal of Physics. – 2020. – No. 3. – P. 81 – 84.

13. **Wachtel, E.** Étude du système Fe-P / E. Wachtel, E. Ubelachker, E. Urbain // Mem. Sci. Rev. Metallurg. – 1964. – Vol. 61, No 7-8. – P. 522 – 524.